Journal of Reinforced Plastics and Composites
http://jrp.sagepub.com/

Thermo-mechanical properties of epoxidized hemp oil-based bioresins and biocomposites

Nathan W Manthey, Francisco Cardona, Gaston Francucci and Thiru Aravinthan

Journal of Reinforced Plastics and Composites published online 26 June 2013

DOI: 10.1177/0731684413493030

Original Article

JOURNAL OF
REINFORCED
PLASTICS &
COMPOSITES

Journal of Reinforced Plastics and Composites
0(00) 1–13

DOI: 10.1177/0731684413493030
jrp.sagepub.com
SAGE

Thermo-mechanical properties of epoxidized hemp oil-based bioresins and biocomposites

Nathan W Manthey[1], Francisco Cardona[1], Gaston Francucci[1,2] and Thiru Aravinthan[1]

Abstract

Novel epoxidized hemp oil-based biocomposites containing jute fibre reinforcement were produced at the Centre of Excellence in Engineered Fibre Composites (CEEFC) owing to the need to develop new types of biobased materials. Mechanical properties (tensile, flexural, Charpy impact and interlaminar shear), thermo-mechanical properties (glass transition temperature, storage modulus and crosslink density) and moisture-absorption properties (saturation moisture level and diffusion coefficient) were investigated and compared with samples containing commercially produced epoxidized soybean oil and a synthetic bisphenol A diglycidyl ether-based epoxy control, R246TX cured with a blend of triethylenetetramine and isophorone diamine. Scanning electron microscopy was also performed to investigate the fibre–matrix interface. Epoxidized hemp oil-based samples were found to have marginally superior mechanical, dynamic mechanical and similar water-absorption properties in comparison to samples made with epoxidized soybean oil bioresin; however, both sample types were limited to bioresin concentrations below 30%. Synthetic epoxy-based samples exhibited the highest mechanical, dynamic mechanical and lowest water-absorption properties of all investigated samples. This study has also determined that epoxidized hemp oil-based bioresins when applied to jute fibre-reinforced biocomposites can compete with commercially produced epoxidized soybean oil in biocomposite applications.

Keywords

Biocomposite, dynamic mechanical analysis, mechanical properties, moisture absorption, natural fibres

Introduction

Increased environmental awareness and focus on sustainability within the fibre composite industry has advanced the development of novel biobased materials. As a result of this, research is being conducted on biocomposites comprising plant oil-based bioresins reinforced with natural fibres or petrochemical-based resins reinforced with plant-based natural fibres. Plant-based natural fibres classified as leaf, bast, fruit, seed, wood, cereal, straw and grass fibres are primarily used as the reinforcement phase in biocomposites.[1,2] Natural fibres provide several key advantages compared with synthetic fibres that justify their use in certain biocomposite applications. They are inexpensive, easy to process, renewable and exhibit high specific material properties with end of life cycle recyclability.[2–4] Plant-based natural fibres also help reduce the carbon footprint of the end composite from the growing of the plants and enhanced energy recovery at the end of their life cycle.[5] The main negative aspects associated with plant-based natural fibres are their

---

[1] Centre of Excellence in Engineered Fibre Composites (CEEFC), Faculty of Engineering and Surveying, University of Southern Queensland, Toowoomba, Queensland, Australia
[2] Composite Materials Group, Research Institute of Material Science and Technology (INTEMA-CONICET), Materials Engineering Department, Engineering Faculty, National University of Mar del Plata, Mar del Plata, Argentina

Corresponding author:
Nathan W Manthey, Centre of Excellence in Engineered Fibre Composites (CEEFC), Faculty of Engineering and Surveying, University of Southern Queensland, Toowoomba, Queensland 4350, Australia.
Email: nathan.manthey@usq.edu.au

Table 1. Mechanical properties of natural fibres compared with E-glass.[7,8]

Fibre	Specific gravity	Tensile strength (MPa)	Young's modulus (GPa)	Specific strength (MPa)	Specific modulus (GPa)
Sisal	1.20	600–700	38	500–583	32
Flax	1.20	800–1500	60–80	667–1250	50–67
Jute	1.46	600–1100	10–30	411–753	7–21
Hemp	1.14	550–900	50–70	482–790	44–62
E-glass	2.60	2000–3400	75	1308	29

hydrophilic nature, low adhesion with polymer matrices, low thermal resistance and variable properties due to differing growing and processing conditions.[2,6] In terms of specific properties, plant-based natural fibres compare favourably with E-glass (Table 1). Due to availability, this study uses jute fibre as the natural fibre reinforcement.

Although using natural fibres indeed enhances the composites 'green' factor, it is imperative that the polymer matrix or a high proportion of it also be of biological origin to move closer to the goal of true 100% biocomposites. One potential way that this can be realized is through the use of plant- or plant oil-based bioresins. Bioresins, in particular plant- or vegetable oil-based bioresins, offer a potential alternative to petrochemical-based resins as the required feedstocks are readily available in most parts of the world.[7] Vegetable oil feedstocks are converted into epoxidized vegetable oil (EVO)-based bioresins through the process of epoxidation. An extensive collection of research involving EVO in terms of synthesis, characterisation and in biocomposite applications has been conducted by many authors.[2,8–30] This research encompasses numerous different vegetable oil feedstocks with the main focus being on soybean, canola and linseed oils. These three oils are also used in food production, which may pose ethical issues. Therefore, to alleviate this conflict of interest, it is important to focus on using fast-growing, non-food oil crops for use as bioresin feedstocks. Due to the numerous diverse fatty acid profiles of different types of non-food vegetable oils, different oil options exist. One such identified type of oil that has shown initial promise is hemp oil.

The Centre of Excellence in Engineered Fibre Composites (CEEFC) is conducting research into the development of novel hemp oil-based bioresins, such as epoxidized hemp oil (EHO) and acrylated epoxidized hemp oil for biocomposite applications.[31–33] Hemp oil is widely considered a by-product of hemp fibre production, with its main uses being in livestock food and pharmaceutical applications. Due to its unique fatty acid profile, high in both linoleic and linolenic acid, hemp oil shows considerable potential as a bioresin feedstock.

In this article, the effect of EHO concentration on the dynamic mechanical behaviour, flexural properties and moisture-absorption of EHO-based bioresin epoxy blends is reported. Comparisons with commercial epoxidized soybean oil (ESO)-based bioresin epoxy blends and a control synthetic epoxy resin are also discussed. EHO-based bioresin epoxy blends applied to jute fibre-based biocomposites are also presented and compared in terms of mechanical properties (tensile, flexural, Charpy impact and interlaminar shear), thermo-mechanical properties (glass transition temperature, storage modulus and crosslink density) and moisture-absorption properties (saturation moisture level and diffusion coefficient) with biocomposite samples prepared using commercially available ESO-based bioresins. Scanning electron microscopy (SEM) was also performed to investigate the fibre–matrix interface. A major motivation for this study is the potential advantage of matching bioresin with natural fibres, as the greater hydrophilic nature of a bioresin versus synthetic epoxy is expected to be more compatible with natural fibres.

Materials

Cold-pressed raw industrial hemp oil supplied by Ecofibre (Maleny, Queensland, Australia) with a fatty acid profile from the supplier's specification sheet consisting of the following acids: palmitic, 6.0%; stearic, 2.0%; oleic, 12.0%; linoleic, 57.0%; linolenic, 20.7%; other, 2.3%, was used for the synthesis of EHO. The provided hemp oil has an iodine number of 165 (g I/100 g oil) and saponification value of 193. Analytical grade glacial acetic acid and hydrogen peroxide with minimum concentrations of 99.7% and 30%, respectively, were used as received from LabServ (Biolab, Australia). Amberlite IR-120 was used as received from Fluka (Sigma-Aldrich, Australia) and was of the ionic H^+ form. A Mettler Toledo LabMax automatic reactor with a 4 l four-necked reaction vessel equipped with a mechanical ‘anchor’ stirrer and thermometer was used for the epoxidation procedure. ESO, oxirane oxygen content 6.8% was used as supplied from Hallstar. Woven jute fibre, 90°/0°, 550 g/m^2, was used as natural fibre reinforcement. No chemical treatments were performed on the fibre. Kinetix R246TX bisphenol A diglycidyl ether-based epoxy resin, EEW $\approx$ 195, isophorone diamine, AHEW $\approx$ 42.6, supplied from ATL composites (Southport, Queensland, Australia) and triethylenetetramine, AHEW $\approx$ 24 (Figure 1), from Huntsman were used as supplied.

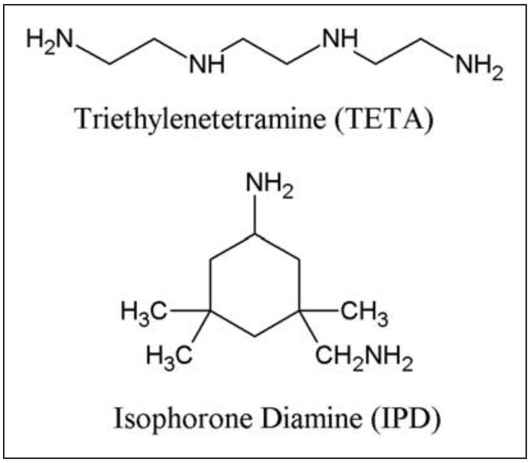

Figure 1. Molecular structures of triethylenetetramine (TETA) and isophorone diamine (IPD).

Experimental

In situ epoxidation of hemp oil

EHO was synthesized through the epoxidation of cold-pressed raw industrial hemp oil (156.25 g, 1 mol) by peroxyacetic acid, formed in situ by the reaction of aqueous hydrogen peroxide (113.4 g, 1 mol) and acetic acid (40.04 g, 0.67 mol) in the presence of an acidic ion exchange resin, Amberlite IR-120 H$^+$ (15% by weight of hemp oil) as the catalyst, as shown in Figure 2. The constituents were added to a four-necked reaction vessel equipped with a mechanical stirrer and a thermometer. Stirring was initiated and the reactor temperature was increased until the mixture reached 40°C, whereby dropwise addition of hydrogen peroxide was performed over a period of 1 h. Temperature and stirring speed were then increased to operational values of 75°C and 110 r/min, respectively. These parameters were maintained for a period of 7 h.

On completion of the reaction, the catalyst was filtered off and the reactor contents were cleaned in a separation funnel by washing thrice with distilled water (cool (~20°C), hot (~85°C), cool (~20°C)) to remove the aqueous phase. Next, the resin was centrifuged and aerated to remove any remaining water. The resin was further dried through the addition of anhydrous sodium sulphate in the proportion of 15 wt% of resin. The water content after drying using a Sartorius MA-50 moisture analyzer was found to be less than 0.3%. Following the addition of anhydrous sodium sulphate, the resin was placed in an oven at 70 C for 12 h and subsequently filtered through Whatman No. 4 filter paper. Oxirane oxygen content was 8.3%, as determined by the direct titration method with hydrobromic acid solution in acetic acid as per earlier studies.[34–36] The yield of EHO bioresin recovered after washing and separation from the catalyst and reactants was approximately 75% by volume in relation to the initial volume of hemp oil. Inevitably, some bioresin was lost during this process of washing and purification. The synthesized EHO has a viscosity of 845 cP compared with the commercial ESO, which was 340 cP. Viscosities were measured at 25°C.

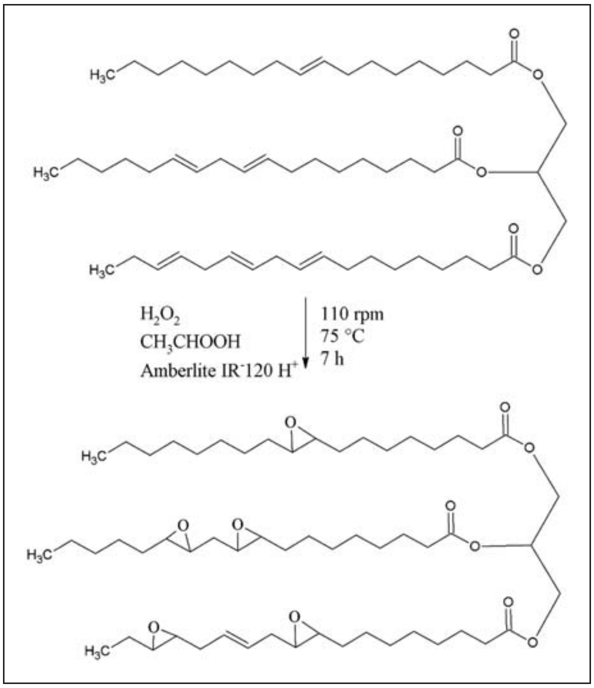

Figure 2. *In situ* epoxidation of hemp oil.

Specimen preparation

EHO- and ESO-based bioresin epoxy blends were prepared by mixing EHO or ESO with a base synthetic epoxy resin, R246TX. The bioresin blends chosen for this study were based on the following weight ratios 0/100%, 10/90%, 20/80%, 30/70% and 40/60% (EHO/R246TX and ESO/R246TX). To produce the bioresin samples, the bioresin blend and hardener were thoroughly mixed, degassed, poured into a waxed mould, cured as outlined below and finally cut to size. Hardener content was adjusted over the range of samples to account for epoxy content so as to ensure consistency.

Flat biocomposite panels were manufactured using the hand lay up process. The lay up consisted of four layers of woven jute mat reinforcement. The fibre was washed with warm water to remove any dust particles and other such contaminants, dried for 12 h at 110°C and finally cut to size. No chemical treatments were performed on the fibre. The manufacture of the composite panels was performed immediately upon removing the fibre from the oven to prevent atmospheric moisture absorption, which could impinge upon the final composite's mechanical properties. Control samples (0/100%) were prepared using synthetic epoxy, R246TX and jute fibre. Manufactured panels measured $300 \times 300 \times 5$ mm with a fibre weight percentage of approximately 20%. A flat metal plate was placed on top of the composite sample to improve the surface finish and to ensure a consistent thickness.

Initial curing for both bioresin and biocomposite samples was performed at room temperature (~25°C) for 4 h followed by post-curing at 120°C for a further 4 h. Following this, the samples were then removed from the mould, cut to size, dried at 80°C for 4 h to ensure the removal of any induced moisture and then cooled in a desiccator ready for testing. An exception to this process was that the water absorption samples were further dried at 110°C for 1 h and cooled in a desiccator as per ASTM D570.

Scanning electron microscopy

Cross-section morphologies of the biocomposite samples were investigated using SEM (JEOL JSM 6460 LV scanning electron microscope, National University of Mar Del Plata, Argentina (UNMdP)). The fractured surfaces were coated with gold and the samples were scanned at room temperature with an accelerating voltage of 15 kV.

Mechanical testing

Interlaminar shear strength (ILSS) testing was performed to determine the effects of bioresin concentration on the fibre–matrix interfacial shear strength. Testing was performed using ISO 14130 on a MTS Alliance RT/10 10 kN machine with a crosshead speed of 1 mm/min.

Charpy impact tests were conducted to determine the effects of bioresin concentration on the impact properties of the biocomposites. Impact properties of the samples were determined using ISO 179 on an Instron Dynatup M14-5162. Charpy impact strength (kJ/m^2) was calculated from equation (1), whereby a_{cU}, h, b and W_B are the Charpy impact strength, thickness, width and the energy at break of the test specimen. Essentially, this corresponds to the energy at break of the specimen divided by the cross-sectional area

$$a_{cU} = \frac{W_B}{bh} \times 10^3 \tag{1}$$

Flexural testing was conducted to determine the behaviour of both bioresin and biocomposite specimens subjected to three-point simple beam loading. Bioresin flexural properties were obtained through three-point bending tests conducted in accordance with ISO 178 using a MTS Alliance RT/10 machine. A crosshead speed of 2 mm/min and a span:depth ratio of 16:1 were used with specimen dimensions being $80 \times 10 \times 4$ mm. Biocomposite flexural properties were measured in accordance with ISO 14125. Tensile tests were conducted in accordance with ISO 527. Tests were performed with a crosshead speed of 2 mm/min using a MTS Insight 100 kN machine. Specimen dimensions were $250 \times 25 \times 5$ mm. Five specimens of each sample type were used in each mechanical test.

Dynamic mechanical analysis

A calibrated TA Instruments Q800 DMA was used for the dynamic mechanical analysis (DMA). Rectangular specimens with dimensions $58 \times 10 \times 5$ mm were tested in dual cantilever mode. Testing was performed at a temperature ramp of 3°C/min over a temperature range of approximately 25–180°C. A frequency of 1.0 Hz with an oscillating displacement of $\pm 10\,\mu$m was also used. Storage modulus (E') and tan δ were plotted as a function of temperature by Universal Analysis 2000 version 3.9 A software. Glass transition temperature (T_g) was calculated as the peak of the tan δ curve and crosslink density (ν_e) was calculated from the theory of rubber elasticity (equation (2)),[37] where E', ν_e, R and T are the storage modulus in the rubbery plateau region (T_g + 40°C), crosslink density, gas constant (8.314 J/(K·mol)) and the absolute temperature in K, respectively.[38]

$$E' = 3\nu_e RT \tag{2}$$

Moisture absorption

Moisture absorption tests were performed in order to ascertain the saturation moisture level and the diffusion coefficient of the bioresin and biocomposite samples.

Specifically the effects of bioresin loading on the moisture absorption were of interest. Testing was performed in accordance with ASTM D570 with three specimens of each sample type being used. Specimens measured $76.2 \times 25.4 \times 5$ mm for both neat resin and jute fibre biocomposite samples. The specimens were cut to size and the edges were finished with No. 0 sandpaper. After this, the specimens were dried at 110°C for 1 h, cooled in a desiccator and weighed to the nearest 0.001 g. The specimens were immersed in distilled water at 23 ± 1°C and removed at regular intervals, wiped free of surface moisture, immediately weighed to the nearest 0.001 g and then replaced in the water. Equation 3 was used to calculate the diffusion coefficient, where D, h, M_m and m are diffusion coefficient, thickness of specimen, saturation moisture level and gradient of the linear region from the plot of weight gain against square time[24]

$$D = \pi\left(\frac{h}{4M_m}\right)m^2 \tag{3}$$

Results and discussion

SEM analysis

In fibre composites, effective wetting and compatibility between the fibre reinforcement and the polymer matrix is paramount in obtaining satisfactory fibre–matrix adhesion and ultimately acceptable end state composite properties. The fracture surfaces of the synthetic epoxy, EHO- and ESO-based jute fibre-reinforced samples were examined by SEM to evaluate the degree of fibre–matrix adhesion; $300\times$ magnification was used to give a representative image of the overall fibre–matrix behaviour, whereas $1000\times$ magnification was used to more closely examine individual fibre–matrix behaviour. Figures 3–8 display the fibre–matrix interface for the synthetic epoxy, EHO- (20/80%) and ESO- (20/80%) based samples. It can be seen that fibre pullout is apparent for all sample types and is visible at $300\times$ magnification. Also apparent is the fibre–matrix interface and the presence of some gaps between the fibre and the matrix. Indeed this fibre–matrix interface condition was anticipated to a certain degree as no chemical treatment was performed on the jute fibre reinforcement. Consequently the conclusions drawn as a result of these findings are reduced fibre–matrix interfacial adhesion with increased EVO content and indicated incompatibility between natural fibre and high concentration EVO/epoxy blends.

Mechanical properties

Samples containing EHO and ESO with jute fibres showed a reduction in ILSS with increasing bioresin

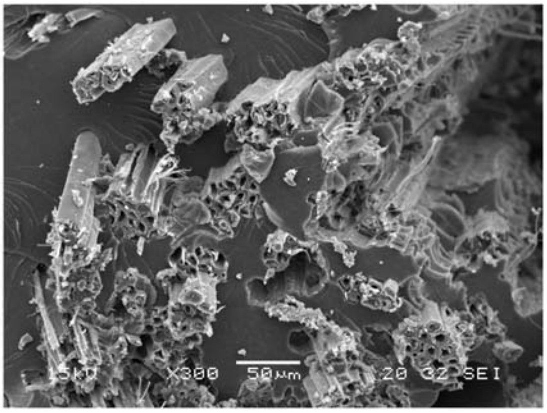

Figure 3. SEM micrograph of synthetic epoxy reinforced jute fibre biocomposite (300×).

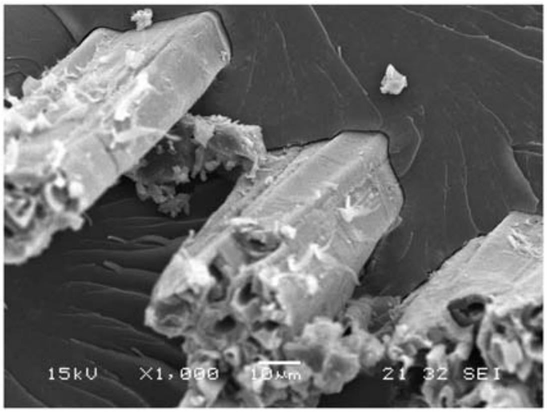

Figure 4. SEM micrograph of synthetic epoxy reinforced jute fibre biocomposite (1000×).

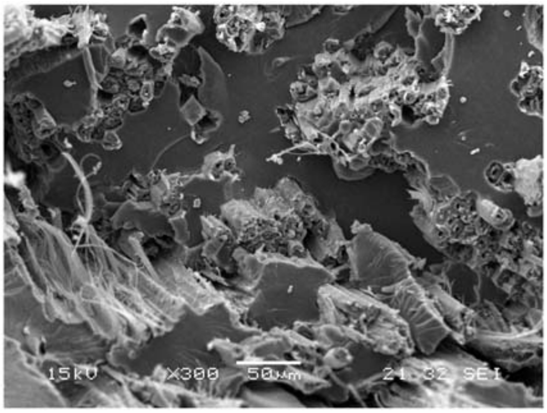

Figure 5. SEM micrograph of EHO synthetic epoxy (20/80%) reinforced jute fibre biocomposite (300×).

Figure 6. SEM micrograph of EHO/synthetic epoxy (20/80%) reinforced jute fibre biocomposite (1000×)

Table 2. Charpy impact and interlaminar shear strength properties of EHO- and ESO jute fibre-based biocomposites.

Bioresin	Charpy impact strength (kJ/m^2)	Interlaminar shear strength (MPa)
R246TX	10.7 ± 1.9	4.3 ± 0.9
ESO 10–90	12.4 ± 2.5	3.4 ± 0.4
ESO 20–80	13.6 ± 3.9	2.6 ± 0.3
ESO 30–70	14.0 ± 3.2	-
ESO 40–60	18.0 ± 6.8	-
EHO 10–90	10.8 ± 0.3	4.1 ± 0.5
EHO 20–80	11.1 ± 0.9	2.7 ± 0.4
EHO 30–70	13.2 ± 1.2	-
EHO 40–60	17.0 ± 6.9	-

EHO: epoxidized hemp oil; ESO: epoxidized soybean oil.

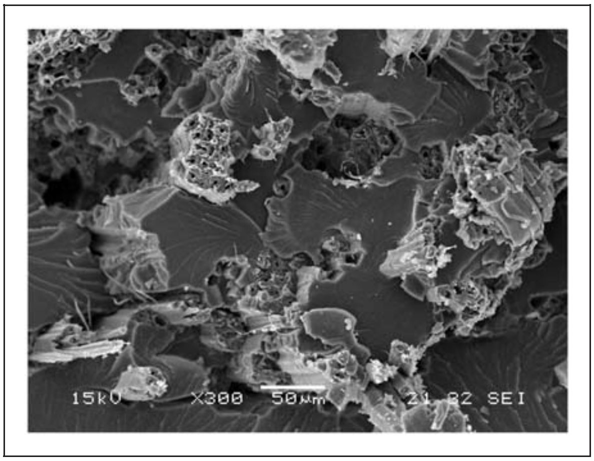

Figure 7. SEM micrograph of ESO/ synthetic epoxy (20/80%) reinforced jute fibre biocomposite (300×).

Table 3. Flexural properties of EHO- and ESO-based bioresin/epoxy blend samples.

Bioresin	Flexural strength (MPa)	Flexural modulus (MPa)
R246TX	108.3 ± 2.9	2359 ± 46
ESO 10–90	79.5 ± 2.6	1905 ± 24
ESO 20–80	74.7 ± 7.6	1895 ± 36
ESO 30–70	61.1 ± 4.9	1490 ± 67
ESO 40–60	3.8 ± 0.2	161 ± 12
EHO 10–90	105.1 ± 9.3	2303 ± 77
EHO 20–80	83.9 ± 2.4	1935 ± 44
EHO 30–70	67.3 ± 0.5	1701 ± 47
EHO 40–60	6.1 ± 1.8	311 ± 33

EHO: epoxidized hemp oil; ESO: epoxidized soybean oil.

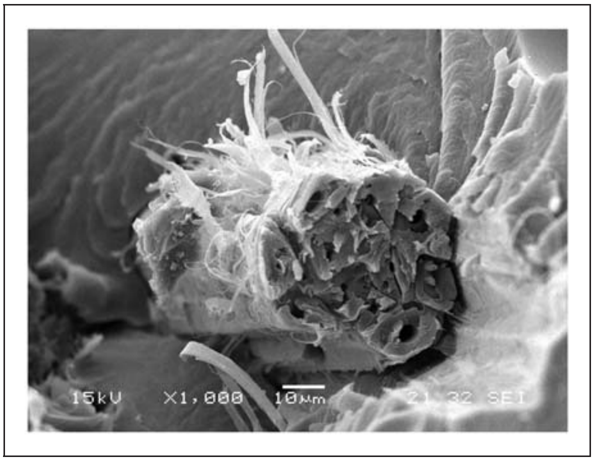

Figure 8. SEM micrograph of ESO/synthetic epoxy (20/80%) reinforced jute fibre biocomposite (1000×).

content (Table 2). Maximum ILSS occurred with the synthetic epoxy with EHO samples displaying slightly higher ILSS than ESO samples throughout the data range. Due to poor ILSS and therefore compromised results, samples after 20% bioresin concentration were not included in the results. The addition of EVO-based bioresin appears to have negative effects on ILSS, indicating reduced fibre–matrix adhesion. A discernible reduction in performance was apparent subsequent to 20% bioresin concentration for both bioresins. These findings indicate that increasing bioresin concentration, especially concentrations above 20%, has negative effects on ILSS.

The fibre–matrix adhesion was found to be lower when the bioresin content was increased, as shown by the ILSS results and reinforced by the SEM images. It is well known that the properties of composite materials

Table 4. Flexural and tensile properties of EHO- and ESO jute fibre-based biocomposites.

Bioresin	Flexural strength (MPa)	Flexural modulus (MPa)	Tensile strength (MPa)	Young's modulus (MPa)
R246TX	66.3 ± 0.8	3129 ± 117	42.5 ± 2.1	4883 ± 142
ESO 10–90	58.3 ± 8.9	2769 ± 122	43.5 ± 1.8	3890 ± 207
ESO 20–80	53.4 ± 3.2	2358 ± 105	30.8 ± 1.5	3334 ± 62
ESO 30–70	34.0 ± 2.6	1781 ± 102	20.9 ± 2.7	2253 ± 43
ESO 40–60	12.5 ± 1.5	689 ± 52	10.5 ± 0.4	1104 ± 77
EHO 10–90	63.7 ± 2.5	3012 ± 169	43.7 ± 3.3	3956 ± 38
EHO 20–80	58.3 ± 2.7	2924 ± 132	38.2 ± 4.4	3470 ± 273
EHO 30–70	49.0 ± 3.9	2475 ± 166	34.2 ± 0.8	3286 ± 22
EHO 40–60	14.5 ± 1.7	864 ± 75	13.7 ± 0.5	1284 ± 65

EHO: epoxidized hemp oil; ESO: epoxidized soybean oil.

are dependent upon the properties of the reinforcement, the properties of the matrix and the characteristics of the matrix/reinforcement interface. Usually, stronger interfaces lead to higher tensile and flexural strengths but reduced impact strength because energy-consuming mechanisms during composite fracture such as fibre pull out are inhibited. Therefore, ILSS results suggest that in addition to the lower strength and higher flexibility of the bioresins, the poor adhesion to the fibres could also have influenced the tensile strength (negatively) and the impact strength (positively).

Examining the results from Table 2 it can also be seen that the Charpy impact strength increased for both EHO and ESO samples with increasing bioresin concentration. This behaviour is attributed to the long fatty acid chains of the EVO imparting flexibility to the matrix thereby increasing the energy required to break the biocomposite samples. Throughout the sample range, ESO samples displayed higher impact strength compared with EHO samples and the control. This is due to the lower crosslink density of the ESO samples compared with EHO and the synthetic control.

Flexural properties for the bioresin and biocomposite samples are shown in Tables 3 and 4, respectively. The highest recorded peak flexural stress and flexural modulus were observed for the synthetic epoxy control sample. At a concentration of 10%, the EHO sample displayed comparable performance to the synthetic epoxy control. Moreover, for both EHO- and ESO-based samples at concentrations greater than 10%, EHO-based samples displayed marginally higher flexural properties than all ESO-based samples. However, it was also noted that there was a marked reduction in flexural properties for both EHO and ESO subsequent to 30% bioresin concentration. A trend of decreasing flexural properties and subsequently increasing ductility for both EHO- and ESO-based samples was observed with increasing bioresin concentration resulting in lower flexural performance. This is in agreement with results obtained by Zhu et al.,[28] who found similar results for ESO/epoxy blends.

EHO-based jute fibre samples displayed comparable peak flexural stress and flexural modulus with the synthetic control up to a concentration of 10% (Table 4 and Figure 9). Both EHO and ESO samples show evidence of decreasing flexural performance with increasing bioresin concentration. Although there is no literature to the author's knowledge regarding this specific biocomposite, there is also limited literature in general pertaining to bioresins with natural fibres. However, in terms of glass fibre reinforcement, these results are in agreement with those found in the literature. For instance, Chandrashekhara et al.[39] manufactured epoxidized allyl soyate (EAS)-based bioresins/epoxy blends reinforced with glass fibre. It was found that an increase in EAS content resulted in a decrease in flexural properties. Espinoza-Perez et al.[19,40] studied the flexural properties of glass fibre-reinforced ESO/epoxy and epoxidized canola oil/epoxy composites. Utilisation of the bioresin blends resulted in reductions in both flexural strength and modulus of 15–86% and 13–65%, respectively, in comparison to the synthetic epoxy control. According to Espinoza-Perez et al.,[19,40] similar results were also realized by Tatlari[41] regarding glass fibre-reinforced ESO/epoxy composites.

When comparing the flexural properties of the neat resin with those of the biocomposites, it was observed that flexural strength was lower in the biocomposites compared with the neat resin. Conversely, the flexural modulus of the biocomposites was found to be higher than the neat resin samples. Given the fact that there is an absence of literature regarding the mechanical properties of EVO-based bioresins and their associated natural fibre-reinforced biocomposites, comparisons are limited. Nonetheless, the addition of the jute fibre reinforcement served to ultimately increase stiffness and consequently brittleness, thereby leading to the results obtained. These results may also be attributed

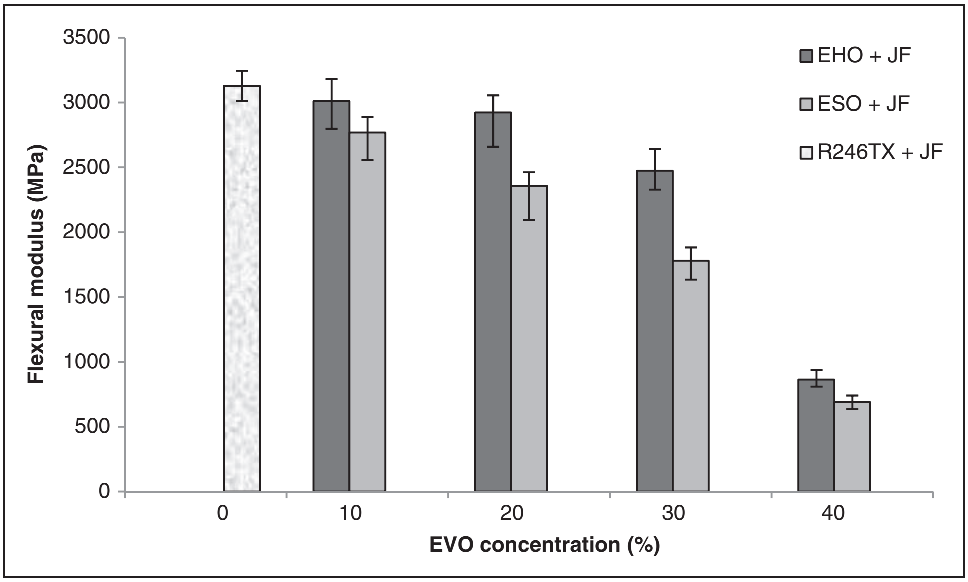

Figure 9. ■■■.

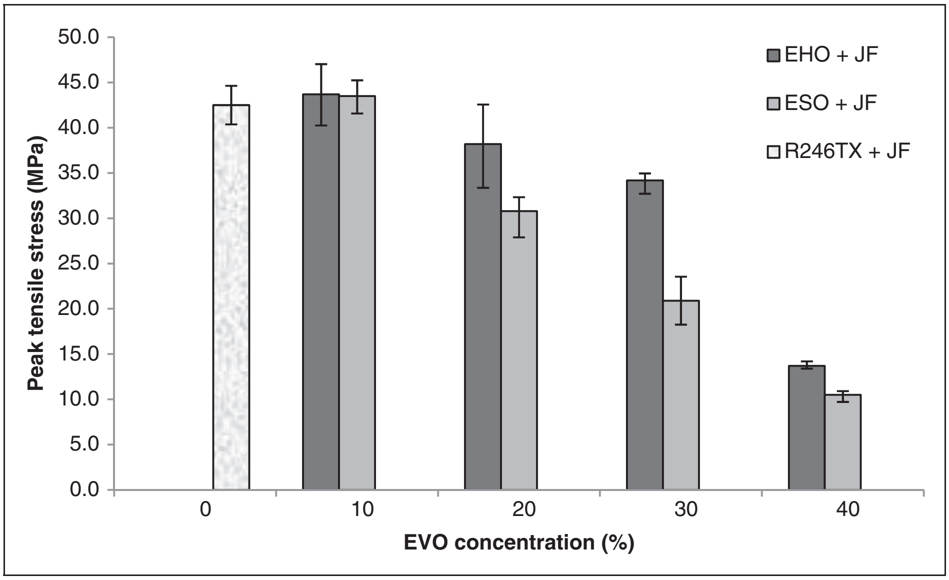

Figure 10. ■■■.

to poor fibre–matrix interfacial adhesion which can be confirmed by ILSS and the associated SEM images.

In contrast with flexural properties, tensile properties are inherently fibre dependant, although the matrix still must be appropriately able to transfer loads to the fibre reinforcement. EHO and ESO jute-based samples displayed similar tensile behaviour at a concentration of 10% bioresin. Samples containing EHO exhibited marginally higher peak tensile stress and modulus of elasticity than ESO samples throughout the intermediate data range (Table 4 and Figure 10). Moreover, both EHO and ESO samples showed lower modulus of elasticity throughout the data range than the control. This behaviour is expected due to the lower modulus of elasticity of EVO-based bioresins and EVO/epoxy blends. Peak tensile stress for both EHO and ESO samples up to a concentration of 10% was greater than the control. Similar results were found by Chandrashekhara et al.[39]

Table 5. Dynamical mechanical properties of EHO- and ESO-based bioresins and biocomposites.

Sample type	Storage modulus at 40°C (MPa)	T_g (°C)	Crosslink density (mol/m^3)
Neat bioresin			
R246TX	1820	107.4	1001
ESO 10–90	1504	93.9	841
ESO 20–80	1401	90.8	623
ESO 30–70	1022	87.7	454
ESO 40–60	185	79.3	62
EHO 10–90	1643	99.1	965
EHO 20–80	1541	96.5	714
EHO 30–70	1170	89.5	418
EHO 40–60	313	80.1	158
Biocomposite			
R246TX	1912	107.1	9936
ESO 10–90	1607	91.4	6599
ESO 20–80	1494	86.1	6252
ESO 30–70	1131	85.2	3601
ESO 40–60	196	76.9	715
EHO 10–90	1770	98.2	6711
EHO 20–80	1599	93.7	5970
EHO 30–70	1244	88.6	4580
EHO 40–60	375	78.6	1427

EHO: epoxidized hemp oil; ESO: epoxidized soybean oil.

in studying the mechanical properties of EAS-based bioresins/epoxy blends reinforced with glass fibre. While no data is presented regarding the tensile strength of said biocomposites, the tensile modulus was found to slightly increase with low levels of bioresin concentration before decreasing with increasing bioresin concentration. It is noted however that lower concentrations of bioresin were used in this study compared to those used within this work.

Dynamic mechanical properties

DMA was performed on bioresin and biocomposite samples in order to characterize the viscoelastic behaviour of both EHO- and ESO-based neat bioresins and biocomposites. Table 5 and Figures 11 and 12 show the effects of EHO and ESO concentration on the storage modulus at 40 C, T_g and crosslink density. For both bioresin and biocomposite sample types, storage modulus was found to decrease with increasing bioresin concentration. Similar behaviour to the flexural properties was observed in that subsequent to 30% bioresin concentration, performance was substantially reduced. The highest recorded storage modulus of the bioresin and biocomposite samples was 1820 and 1912 MPa, respectively, for the synthetic epoxy control samples. Samples containing EHO displayed higher storage modulus than those containing the same concentration of ESO.

The T_g of EHO and ESO bioresin samples was determined from the peak of the tan δ curve using Universal Analysis 2000 version 3.9 A software. Commonly a higher T_g is obtained when the bioresin component has a lower epoxide equivalent weight (EEW) and higher epoxy functionality.[42] This was apparent and expected in this study as EHO has a lower EEW and higher epoxy functionality compared with ESO and consequently displayed higher T_g values than ESO samples throughout the data range. The change in T_g for the bioresin compared with the biocomposite samples was found to be negligible. Of all the different samples, the synthetic epoxy control was found to exhibit the highest T_g of 107.4°C. The relationship between bioresin concentration and T_g was found to be approximately linear, thereby supporting the findings of Miyagawa et al.[38] A reduction in T_g was observed with increasing bioresin content, which is also in agreement with results found by Espinoza-Perez et al.[19] and Miyagawa et al.[38]

Crosslink density is also outlined in Table 5. Similar to the storage modulus and the T_g values, the value of the crosslink density was found to decrease with increasing bioresin concentration. These findings are again consistent to those of Miyagawa et al.[38,42] As expected, the synthetic epoxy control sample exhibited the highest crosslink density. EHO samples displayed higher crosslink density than ESO samples at the same bioresin concentrations. Subsequent to 30% bioresin concentration, the crosslink density markedly decreased, suggesting that synthetic epoxy replacement is limited to lower bioresin concentrations. Both EHO and ESO were found to be non-transparent above 30% concentrations. This non-transparency is the result of differences between reactivity of the terminal epoxy groups in the synthetic resin and the epoxy groups located centrally in the bioresin towards the amine curing agent. Crosslink densities were found to be higher for biocomposites samples in comparison to the neat bioresin samples primarily due to improved storage moduli. Similar results were found by Jacob et al.[43] and Rahman et al.,[44] who found increased crosslink densities of composites in comparison to those of neat resin samples.

Moisture absorption

Akil et al.[45] mentioned three different mechanisms acting in the moisture absorption of fibre-reinforced composites, namely, diffusion of water molecules inside the microgaps between polymer chains, capillary

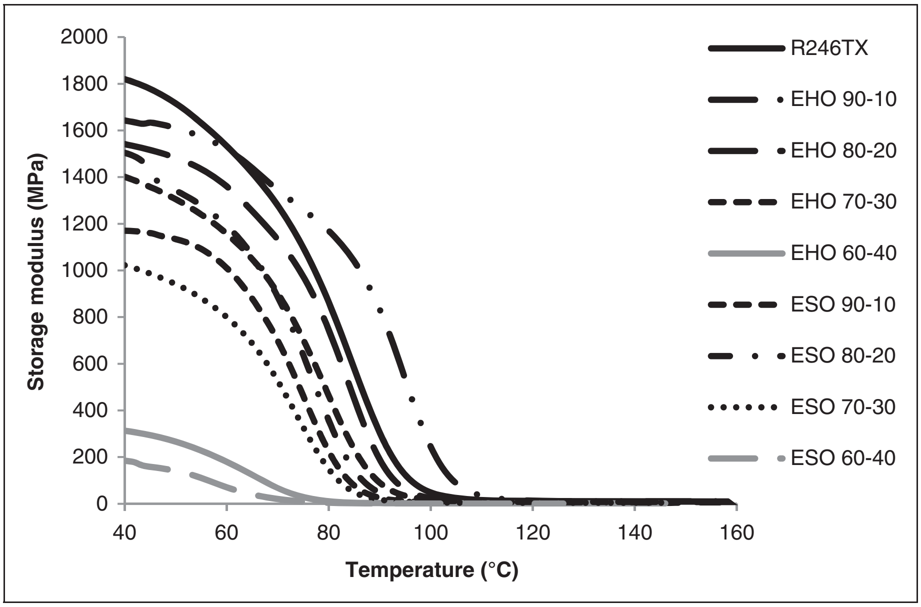

Figure 11. ■■■.

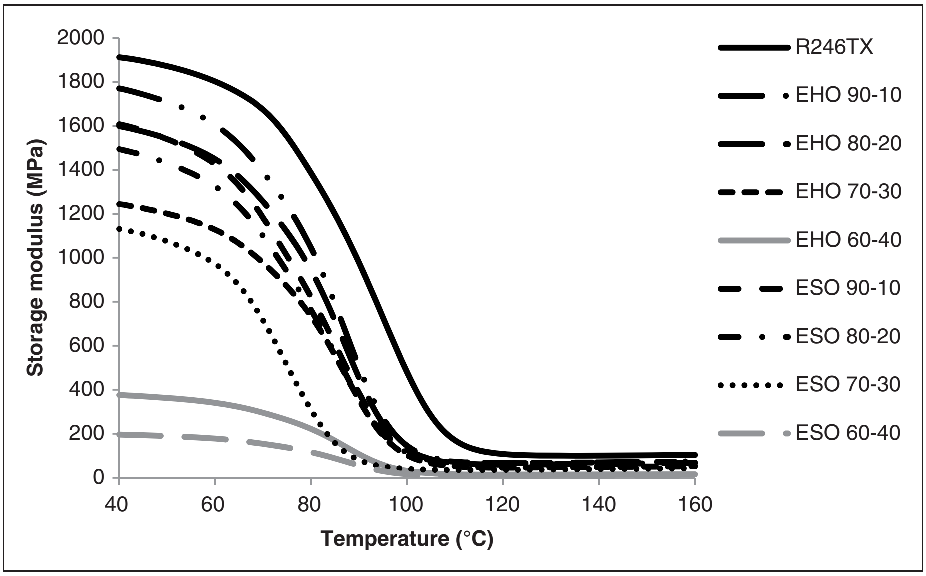

Figure 12. ■■■.

transport into the gaps and flaws of the interfaces between fibre and the matrix and transport through microcracks in the matrix arising from fibre swelling (particularly in the case of natural fibre composites). Moreover, the hydrophilic temperament of natural fibres increases moisture absorption of the final composites.

The moisture absorption results obtained in this study showed that the biocomposites immersed in distilled water at 23.1°C followed a linear Fickian behaviour, whereby the moisture weight gains gradually reached equilibrium after a rapid initial phase. Moisture absorption data, specifically diffusion coefficient and saturation moisture content of the bioresin blends and jute fibre-reinforced biocomposites is shown in Table 6. The moisture absorption of the epoxy bioresin blends and biocomposite samples was found to increase with increased bioresin loading.

Table 6. Water-absorption properties of EHO- and ESO-based bioresin/epoxy blends and biocomposites.

Sample type	Diffusion coefficient × 10^{-6} (mm^2/s)	Saturation moisture content (%)
Bioresin samples		
R246TX	1.78	1.05
EHO 20–80	1.85	1.22
ESO 20–80	1.93	1.26
EHO 40–60	1.99	1.47
ESO 40–60	2.03	1.51
Jute fibre samples		
R246TX	4.24	9.32
EHO 20–80	4.60	15.20
ESO 20–80	4.70	16.63
EHO 40–60	5.09	24.13
ESO 40–60	5.46	25.71

EHO: epoxidized hemp oil; ESO: epoxidized soybean oil.

This behaviour was also reported by Tan and Chow[46] for epoxidized palm oil blends.

As previously stated, fibres provide an additional transport mechanism for water transport throughout the material and therefore the composite water uptake was always higher than that observed for the neat resin samples. As expected, the highest moisture absorption was shown by the jute fibre biocomposite samples. These fibres dramatically increase both the diffusion coefficient and saturation moisture content of the composites as they absorb water as a consequence of their hydrophilic nature given by the hydroxyl groups in the cellulose component of the fibres and swell, allowing the transport of water along microcracks in the matrix arising from the swelling of fibers.[24] EHO-based samples displayed marginally lower diffusion coefficient sand saturation moisture contents than ESO-based samples, although the difference is insignificant.

Conclusions

EHO-based bioresins and jute fibre-reinforced biocomposites were manufactured and compared with ESO-based samples in terms of SEM, mechanical, dynamic mechanical and water-absorption properties. EHO-based biocomposite samples were found to display marginally higher tensile stress, modulus of elasticity, flexural stress, flexural modulus and ILSS than ESO-based samples. Mechanical performance decreased for both EHO and ESO bioresins and biocomposites with increased bioresin loading. A significant reduction occurred after 30% bioresin concentration. As expected, synthetic epoxy control samples displayed superior mechanical performance compared with both EHO and ESO samples. From the SEM analysis it was confirmed that fibre–matrix interfacial adhesion was negatively affected with increasing bioresin content. Therefore, future work will involve studying different fibre chemical treatments, such as alkai treatment with the aim of improving fibre–matrix adhesion.

Overall, this study has shown that EHO-based bioresins when applied to jute fibre-reinforced biocomposites can compete with commercially produced ESO in terms of mechanical performance, dynamic mechanical properties and water-absorption characteristics. However, the general, realistic conclusion is that both EHO and ESO are indeed best suited to a plasticizing role rather than complete bioresin matrices, although it was shown that EHO can be used in marginally higher concentrations than ESO.

Funding

The authors would like to thank the Queensland State Government for providing a Smart Futures PhD Scholarship, the Australian Government for providing an Endeavour Research Award and the National Scientific and Technical Research Council of Argentina (CONICET), which provided financial support for this research work.

Acknowledgement

Thanks are extended to Mr Wayne Crowell for providing technical support.

References

1. John MJ and Thomas S. Biofibres and biocomposites. *Carbohydrate Polym* 2008; 71: 343–364.
2. O'Donnell A, Dweib MA and Wool RP. Natural fiber composites with plant oil-based resin. *Compos Sci Technol* 2004; 64: 1135–1145.
3. Agrawal R, Saxena NS, Sharma KB, et al. Activation energy and crystallization kinetics of untreated and treated oil palm fibre reinforced phenol formaldehyde composites. *Mater Sci Eng A* 2000; 277: 77–82.
4. Canché-Escamilla G, Cauich-Cupul JI, Mendizábal E, et al. Mechanical properties of acrylate-grafted henequen cellulose fibers and their application in composites. *Compos Part A: Appl Sci Manufac* 1999; 30: 349–359.
5. Joshi SV, Drzal LT, Mohanty AK, et al. Are natural fiber composites environmentally superior to glass fiber reinforced composites? *Compos Part A: Appl Sci Manufac* 2004; 35: 371–376.
6. Saheb DN and Jog JP. Natural fiber polymer composites: a review. *Adv Polym Technol* 1999; 18: 351–363.
7. Wool R and Sun X. *Bio-based polymers and composites*, 1st ed. Oxford: Academic Press, 2005.
8. Adekunle K, Åkesson D and Skrifvars M. Biobased composites prepared by compression molding with a novel thermoset resin from soybean oil and a natural-fiber reinforcement. *J Appl Polym Sci* 2010; 116: 1759–1765.

9. Adekunle K, Åkesson D and Skrifvars M. Synthesis of reactive soybean oils for use as a biobased thermoset resins in structural natural fiber composites. *J Appl Polym Sci* 2010; 115: 3137–3145.
10. Bouchareb B and Benaniba MT. Effects of epoxidized sunflower oil on the mechanical and dynamical analysis of the plasticized poly(vinyl chloride). *J Appl Polym Sci* 2008; 107: 3442–3450.
11. Can E, Wool RP, Küsefoğlu S, et al. Soybean and castor oil based monomers: synthesis and copolymerization with styrene. *J Appl Polym Sci* 2006; 102: 2433–2447.
12. Can E, Wool RP, Küsefoğlu S, et al. Soybean- and castor-oil-based thermosetting polymers: mechanical properties. *J Appl Polym Sci* 2006; 102: 1497–1504.
13. Chandrashekhara K, Flanigan V, Berring N, et al. Pultrudable resin from soybean oil. In: *Proceedings of the 44th international SAMPE symposium and exhibition*, Long Beach, CA, 23–27 May 1999, pp. 1857–1865.
14. Czub P. Application of modified natural oils as reactive diluents for epoxy resins. *Macromol Symp* 2006; 242: 60–64.
15. Czub P. Characterization of an epoxy resin modified with natural oil-based reactive diluents. *Macromol Symp* 2006; 245-246: 533–538.
16. Dweib MA, Hu B, Shenton III HW, et al. Bio-based composite roof structure: manufacturing and processing issues. *Compos Struct* 2006; 74: 379–388.
17. Espinoza-Pérez J, Wiesenborn D, Haagenson D, et al. Study of the process parameters of the canola oil epoxidation.In: *ASABE annual international meeting*, Providence, RI, 29 June–2 July 2008.
18. Espinoza-Pérez J, Wiesenborn D, Kristi T, et al. Preparation and partial characterization of canola-based epoxy resins for bio-based plastic composites. In: *ASABE annual international meeting*, Minneapolis, MN, 17–20 June 2007.
19. Espinoza-Pérez J, Wiesenborn D, Ulven C, et al. Epoxy resins from high-oleic oils applied to composites. In: *ASABE annual international meeting*, Reno, NV, 21–24 June 2009.
20. Hong CK and Wool RP. Development of a bio-based composite material from soybean oil and keratin fibers. *J Appl Polym Sci* 2005; 95: 1524–1538.
21. Jin F-L and Park S-J. Thermomechanical behavior of epoxy resins modified with epoxidized vegetable oils. *Polym Int* 2008; 57: 577–583.
22. Khot SN, Lascala JJ, Can E, et al. Development and application of triglyceride-based polymers and composites. *J Appl Polym Sci* 2001; 82: 703–723.
23. Meyer P, Techaphattana N, Manundawee S, et al. Epoxidation of soybean oil and jatropha oil. *Thammasat Int J Sci Technol* 2008; 13: 1–5.
24. Morye SS and Wool RP. Mechanical properties of glass/flax hybrid composites based on a novel modified soybean oil matrix material. *Polym Compos* 2005; 26: 407–416.
25. Park S-J, Jin F-L and Lee J-R. Synthesis and thermal properties of epoxidized vegetable oil. *Macromol Rapid Commun* 2004; 25: 724–727.
26. Petrovic ZS, Zlatanic A, Lava CC, et al. Epoxidation of soybean oil in toluene with peroxoacetic and peroxoformic acids - kinetics and side reactions. *Eur J Lipid Sci Technol* 2002; 104: 293–299.
27. Takahashi T, Hirayama K-i, Teramoto N, et al. Biocomposites composed of epoxidized soybean oil cured with terpene-based acid anhydride and cellulose fibers. *J Appl Polym Sci* 2008; 108: 1596–1602.
28. Zhu J, Chandrashekhara K, Flanigan V, et al. Curing and mechanical characterization of a soy-based epoxy resin system. *J Appl Polym Sci* 2004; 91: 3513–3518.
29. Tan SG and Chow WW. Thermal properties, curing characteristics and water absorption of soybean oil-based thermoset. *Polym Lett* 2011; 5: 480–492.
30. Wang R and Schuman TP. Vegetable oil-derived epoxy monomers and polymer blends: a comparative study with review. *Polym Lett* 2013; 7: 272–292.
31. Manthey NW, Cardona F and Aravinthan T. Mechanical properties of epoxidized hemp oil based biocomposites: preliminary results. In: *The first international postgraduate conference on engineering, designing and developing the built environment for sustainable wellbeing* (ed Cowled C), Brisbane, Queensland, 2011. Queensland: Queensland University of Technology, pp. 100–105.
32. Manthey NW, Cardona F, Aravinthan T, et al. Cure kinetics of an epoxidized hemp oil based bioresin system. *J Appl Polym Sci* 2011; 122(1): 444–451.
33. Manthey NW, Cardona F, Aravinthan T, et al. Natural fibre composites with QLD based fibres and vegetable oils. In: *21st Australasian conference on the mechanics of structures and materials: incorporating sustainable practice in mechanics of structures and materials (ACMSM21)*, (eds Fragomeni S, Venkatesan S, Lam N and Setunge S), Victoria, Melbourne, Australia, 7–10 December 2010. Balkema, The Netherlands: CRC Press, pp. 469–473.
34. Dinda S, Patwardhan AV, Goud VV, et al. Epoxidation of cottonseed oil by aqueous hydrogen peroxide catalysed by liquid inorganic acids. *Biores Technol* 2008; 99: 3737–3744.
35. Goud V, Patwardhan A, Dinda S, et al. Epoxidation of karanja (*Pongamia glabra*) oil catalysed by acidic ion exchange resin. *Eur J Lipid Sci Technol* 2007; 109: 575–584.
36. Goud V, Patwardhan A and Pradhan N. Kinetics of *in situ* epoxidation of natural unsaturated triglycerides catalyzed by acidic ion exchange resin. *Ind Eng Chem Res* 2006; 46: 3078–3085.
37. Shabeer A, Chandrashekhara K and Schuman T. Synthesis and characterization of soy-based nanocomposites. *J Compos Mater* 2007; 41: 1825–1849.
38. Miyagawa H, Mohanty A, Misra M, et al. Thermophysical and impact properties of epoxy containing epoxidized linseed oil - Amine-cured epoxy. *Macromol Materi Eng* 2004; 289: 636–641.
39. Chandrashekhara K, Sundararaman S, Flanigan V, et al. Affordable composites using renewable materials. *Mater Sci Eng: A* 2005; 412: 2–6.
40. Espinoza-Pérez J, Wiesenborn D, Tostenson K, et al. Canola-based epoxy resins applied to plastic composites.

In: *2007 ASABE/CSBE north central intersectional conference*, Fargo, North Dakota, USA, 2007.

41. Tatlari M. *Vegetable oil-based epoxy resin for structural composite material manufacturing*. Fargo: North Dakota State University, 2008.
42. Miyagawa H, Misra M, Drzal LT, et al. Fracture toughness and impact strength of anhydride-cured biobased epoxy. *Polym Eng Sci* 2005; 45: 487–495.
43. Jacob M, Francis B, Thomas S, et al. Dynamical mechanical analysis of sisal/oil palm hybrid fiber-reinforced natural rubber composites. *Polym Compos* 2006; 27: 671–680.
44. Rahman MM, Zainuddin S, Hosur MV, et al. Effect of NH2-MWCNTs on crosslink density of epoxy matrix and ILSS properties of e-glass/epoxy composites. *Compos Struct* 2013; 95: 213–221.
45. Akil HM, Cheng LW, Mohd Ishak ZA, et al. Water absorption study on pultruded jute fibre reinforced unsaturated polyester composites. *Compos Sci Technol* 2009; 69: 1942–1948.
46. Tan SG and Chow WS. Thermal properties, fracture toughness and water absorption of epoxy-palm oil blends. *Polym-Plastics Technol Eng* 2010; 49: 900–907.